Effect of Hydrolysis on Porosity of Cellulose Acetate Reverse Osmosis Membranes

K. KOŠUTIĆ, B. KUNST

Faculty of Chemical Engineering and Technology, University of Zagreb, 10000 Zagreb, Croatia

Received 13 July 2000; accepted 7 October 2000

ABSTRACT: The alkaline hydrolysis of asymmetric cellulose acetate membranes was investigated. The changes of cellulose triacetate and cellulose diacetate membrane performances caused by hydrolysis of the membrane material were measured, and the data were analyzed in terms of pore size distributions and effective number of pores in the upper membrane layer before and after hydrolysis. The resulting membranes rejection factors decrease of 10–25%, and a noticeable permeation rates increase were caused by closing of a part of the smallest "network" membrane pores and by increasing the size of the other pores. © 2001 John Wiley & Sons, Inc. J Appl Polym Sci 81: 1768–1775, 2001

Key words: asymmetric membranes; cellulose acetates; hydrolysis; pore size distribution; membrane performance

INTRODUCTION

Reverse osmosis and ultrafiltration membranes made of cellulosics for water desalination and purification purposes today are mostly replaced by polymer thin-film composite membranes. The cellulosic materials are still used for the preparation of membranes for various industrial applications and specific purposes owing to their low price and a long and useful experience in making the good membranes of tailored properties. One of the most promising cellulosic materials[1] suitable for the preparation of successful asymmetric separation membranes is cellulose triacetate (CTA), cellulose ester with 43.7 wt % acetyl content. CTA was known to be superior to the most often used cellulosic membrane material, cellulose diacetate (CDA), the ester with 39.8 wt % of acetyl, due to its better hydrolytic stability and a great resistance to free chlorine and biodegradation. The main obstacle to use it widely for the asymmetric membrane making by the phase separation method has been its poor solubility in solvents miscible with water.

The membrane stability in case of the cellulose ester membranes is usually related to its stability against hydrolysis. A detailed mechanism of the asymmetric cellulose acetate membrane hydrolysis is not yet available. The early studies by Voss et al.[2] on highly porous cellulose acetate membrane hydrolysis showed that, after an ill-defined induction period, the changes in membrane water and salt permeabilites followed the first-order kinetics. Sammon et al.[3] proposed two mechanisms for the overall hydrolysis rate. The first mechanism assumes that the hydrolysis rate is the greatest at the membrane surface and changes in the membrane material caused by hydrolysis are the result of a hydroxyl ion concentration front moving progressively through the membrane. In the second mechanism, the hydroxyl ion concentration and consequently the hydrolysis rate were assumed to be essentially constant throughout the membrane. However, experimental evidences

Correspondence to: B. Kunst.

Journal of Applied Polymer Science, Vol. 81, 1768–1775 (2001)

Table I Membrane Casting Dope Compositions (wt %)

Dope Type	CTA	CDA	Dioxane	Acetone	Methanol	Maleic Acid	$Mg(ClO_4)_2$	Water
T	13.0	—	56.1	22.5	3.6	4.8	—	—
D	—	17.0	10.0	59.2	—	—	1.45	12.35

to check the validity of the mechanisms proposed were not provided. Other investigators[4,5] related changes in membrane transport behavior to changes in acetyl content of the membrane leading to the conclusion that changes in transport behavior might be used as a measure of the hydrolysis reaction. McCray et al.[6] concluded that hydrolysis of an asymmetric membrane with a density gradient throughout the membrane is more complicated than hydrolysis in a dense membrane layer. It was not clearly determined what was the most important step on the inside of the membrane, internal mass transfer or/and chemical reaction control.

It therefore seemed appropriate to apply some new developments in the membrane characterization to bring more light to changes in cellulosic membranes caused by hydrolysis. One of such development is a method of porosity characterization introduced earlier[7–10] and modified and tested recently[11,12]. By this method, a pore size distribution (PSD) and the effective number of pores in the membrane upper layer were determined. If used for the characterization of the membranes before and after partial hydrolysis the method could show the effect of hydrolysis on the porosity of the membrane's skin, a part of the asymmetric membrane structure decisive for the overall selectivity and productivity of the membrane.

The aim of this work was to measure the changes taking place in the performance of CTA and CDA asymmetric membrane samples as a result of hydrolysis of cellulose acetate membrane material, and to correlate these changes to variations in the pore size distribution and effective number of pores determined in the skin of the used membranes.

EXPERIMENTAL

Membranes

Cellulose triacetate (Hercules Ltd, London), type TH 22 with 43.4 wt % of acetyl, and cellulose diacetate, Eastman grade 398-3 with 39.8 wt % of acetyl, and reagent-grade solvents and additives were used. The membranes were prepared from the casting dopes of compositions shown in Table I. Membrane casting dopes are supposed to be homogeneous, clear, gel- and fiber-free solutions. In CTA systems containing $\leq$15 wt % of polymer, this is not the case. The fairly concentrated CTA "solutions" are highly viscous, not quite transparent, and not completely gel-free. Therefore they were homogenized before casting in a high-shear homogenizer (Bioblock Scientific), type H87247, France, for half an hour, left standing thereafter for air bubbles to come out, put into an ultrasound bath for half an hour and finally cast.

The polymer solutions were cast on the clean glass plates using a Gardener knife adjusted to a gap of 0.25 mm. Temperature of both the casting dope and casting atmosphere was 25°C, and the relative humidity of the surrounding air was 60–65%. The solvent evaporation period was 30 s. After solvent evaporation the glass plate with the cast layer was immediately immersed into a gelation bath consisting of ice-cold water.

Membrane testing

The membranes were tested in the reverse osmosis setup described earlier.[12] All the membranes were prepressurized at 22 bar for 2 h. The reverse osmosis experiments were carried out at laboratory temperature and pressure of 17.0 bar, using a sodium chloride and organic reference solutes (markers) solution as a feed. The feed concentration in case of sodium chloride solution was 3500 ppm, and in case of marker solutions 100 ppm. The following organic markers were used: 1,3-dioxolane, 1,4-dioxane, oxepane, 12-Crown-4, 15-Crown-5, and 18-Crown-8.

In each experiment, pure water flow rates Q_w, solution permeate flow rates Q, and rejection factors R were determined. The pure water flow rate Q_w and the solution permeate flow rate Q refer to the mass of the permeate through a unit surface area of a membrane and in a unit time (kg m^{-2}

h^{-1}) corrected to 25°C. The dimensionless membrane rejection factor R, defined as

$$R = 1 - \frac{C_p}{C_f}$$

where C_p and C_f are permeate and feed concentrations (ppm), respectively.

The sodium chloride concentrations were determined by conductivity measurements, and those for the markers by Carbon analyzer, model 1555, Ionics, Inc.

Hydrolysis

The best membrane stability data against hydrolysis are obtained from a long- term dynamic operation of the membrane on the test solution. This approach takes an excessive amount of time. The membrane stability can also be evaluated by accelerated degradation of the membrane material by exposing the samples to hydrolytic solutions in various soak tests, but the data have never been wholly satisfactory. It is preferable to perform accelerated testing in a test cell, using the same piece of the membrane, to avoid difficulties in obtaining meaningful "before" and "after" test data. Although such a method does not replace actual time-dynamic test, it does, however, provide a quick means of determining necessary relative stability data.

The previously characterized cellulose acetate membranes in this work were hydrolyzed by pumping the sodium bicarbonate/sodium carbonate buffer solution of pH 10 in reverse osmosis cells under the pressure of 17 bar to permeate the buffer solution through the membranes. After 10 min of pumping, the membranes were left soaked in the buffer solution for 90 h with four more 10-min periods of pumping the alkaline solution. The whole setup was then thoroughly washed with distilled water and the hydrolyzed membranes were characterized again by permeating the sodium chloride and the markers' solutions.

Pore Size Distribution Calculation

The concept and details of the calculation procedure are given in the earlier papers.[11,12] They are based on the surface force-pore flow (SF-PF) model of material transport through a membrane[7] and experimentally obtained solute rejections for a number of markers. The surface force-pore flow (SF-PF) model takes into account interaction forces between the membrane surface and the solute, expressed by an electrostatic or a Lennard–Jones type potential function, and the solute and solvent transport through the membrane under the influence of such forces. During calculation, pertinent quantities, such as permeation volume, permeation rate, solute concentration at the pore outlet, and solute rejection for a single pore, were defined. By adding up these quantities for a collection of pores the permeation rate and the solute rejection factor values of various markers were computed as functions of the pore size distribution through the collection of active pores. The results were finally compared with experimental data to give the best-fit pore size distribution in the membrane's skin. In addition to pore size distribution, the effective number of pores in the membrane's skin were calculated using this method.

The experimental data on the rejection factors of the markers used throughout the PSD calculation are given in Tables A1 and A2 in the Appendix.

RESULTS AND DISCUSSION

The results of membrane performance testing, using a sodium chloride solution both before and after hydrolysis, are given in Table II.

A comparison of the performance data for all the examined membranes before hydrolysis, shown in the left part of Table II, points first to the differences in their productivities expressed by the Q_w and Q values. These values of membranes T1, T8, and D1 were lower than those of T2 and D2 films. The rejection factor values R were just about the same for membranes T1, T2, and D2, with a slightly higher R value of the membrane D1, and the slightly lower R value of membrane T8. Such results confirm the known fact that the membranes from the same lot as a rule have the same selectivity expressed by the rejection factor, and can vary significantly in their productivity.

The performance data of the membranes after the hydrolysis shown in the right half of Table II indicate a pronounced effect of the hydrolysis process to the membranes' behavior. The results show that the sodium chloride rejection factor values for all the investigated membranes remarkably decreased. This was accompanied by

Table II Membrane Performance Data Using Sodium Chloride Solutions

	Before Hydrolysis			After Hydrolysis		
	Q_w (kg/m^{2}h)	Q (kg/m^{2}h)	R	Q_w (kg/m^{2}h)	Q (kg/m^{2}h)	R
T1	45.0	35.8	0.864	46.1	38.4	0.779
T2	59.9	46.2	0.876	62.3	52.0	0.782
T3	44.3	37.2	0.838	47.0	43.4	0.664
D1	43.6	35.1	0.913	47.7	39.5	0.785
D2	61.8	49.8	0.861	65.7	60.8	0.657

the slight increase of the pure water flow rates Q_w and solution permeate flow rates of sodium chloride solutions Q for all the membranes.

The observed membrane performance variations caused by hydrolysis originate from changes in the membranes' porosity. It is well known that the membrane performance parameters, rejection factor and permeate flux, are influenced by membrane characteristics, primarily its porosity, by physicochemical properties of the system, and by operating variables such as solute concentration and operating pressure. Keeping all the other parameters constant, the change in membranes' porosity, expressed by the pore size distribution (PSD) and effective number of pores in the upper layer of the membrane, would provide experimental evidence for the observed rejection factors and permeate flux changes.

It should be noted here that the term "pore" in this work is conceived as polymer material-free void space through which fluid transport can take place under a driving force. The pores in a dense membrane skin may be envisaged as voids in the membrane material <1 nm in diameter that are formed naturally in solid polymers. Such pores or density defects are caused by the irregular packing of almost randomly kinked stiff-chain molecules. They can also be created by local internal contraction in a crystallizable polymer during the crystallization process. The pores can be circular and noncircular in shape, open or closed, and may or may not form continuous and interconnecting network. The porous membrane skin structure can also be changed during postformation membrane treatments (annealing, swelling, pressurizing); during long use; and in an acid, alkaline, and oxidizing conditions.

The results of the pore size distribution determination for the investigated membrane samples before hydrolysis are shown in Figure 1. The results presented in Figure 1 show that PSD curves of both membrane types are at least bimodal, and some are even trimodal. This confirms the earlier finding of the occurrence of basically two distinct distributions of pore sizes on the membrane surface, named "polymer network" pores and "polymer aggregate" pores.[10] The PSD curves of cellulose triacetate membranes appear often to be trimodal (e.g., of membranes T1 and T3) differing obviously from bimodal PSD of the cellulose diac-

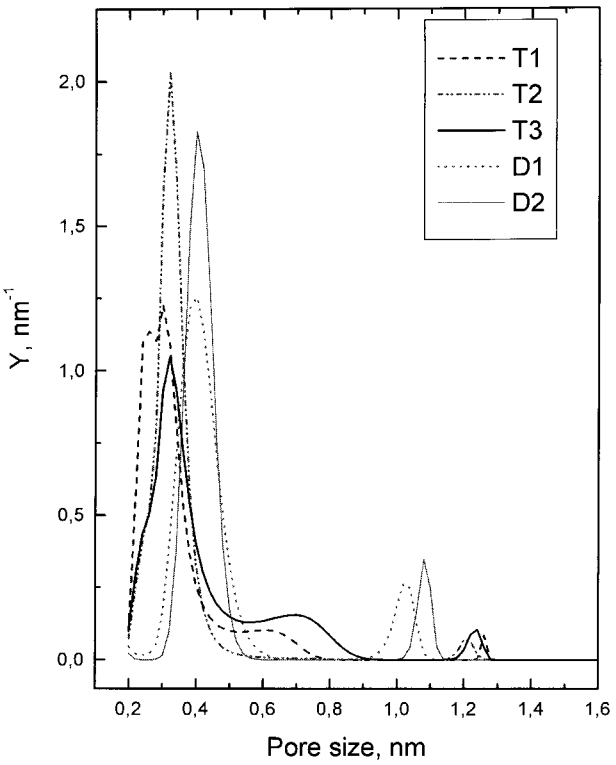

Figure 1 Pore size distributions of the membrane samples before hydrolysis.

Table III Effective Number of Pores *N* in Examined Membrane Skin Before and After Hydrolysis

$N/10^{16}$ m^{-2}	Before Hydrolysis	After Hydrolysis
T1	1.285	0.452
T2	1.416	0.677
T3	0.807	0.572
D1	0.876	0.461
D2	1.134	0.671

etate membranes. The first main maxima of the PSD of the CTA membranes are located at the small pore size of ~0.3 nm and the second much lower maxima are found at nanosize dimensions, 1.20, 1.24, and 1.26 nm, respectively. The very low second maxima indicate small fractions of the aggregate pores, meaning that the small network pores make most of the pores in the CTA membrane skin.

Some differences among the PSD of the three CTA membrane samples are also visible. The first peak of the T1 membrane consists of two overlapping distributions with maxima located at 0.25 and 0.3 nm, and there is a horizontal part of the PSD curve between 0.46 and 0.62 nm, indicating the existence of a certain amount of medium-size pores. In the PSD of the T3 membrane, even greater fraction of the medium-size pores, between 0.46 and 0.75 nm, appears; the smallest, network pores maximum is the lowest of all the CTA membranes. The PSD of the T2 membrane is bimodal with the highest network pores maximum and without medium-size pores.

The pore size distributions of the CDA membranes are purely bimodal. The first, main maxima are found at the larger pore size, at 0.4 nm, and the second distribution is above 1 nm, but at the lower pore size than those for CTA membranes, between 1.0 and 1.1 nm. The second maxima are remarkably higher than those of the CTA membranes indicating a greater fraction of the large, aggregate pores in the skin of the CDA membranes.

The presented pore size distributions should be considered in conjunction with the calculated effective number of pores in the membranes' skin that are given in the first column of Table III. The order of the *N* values listed is:

$$T2 > T1 > D2 > D1 > T3$$

which is almost the same order as that of the maxima of the network (smaller) pores distribution in the membrane PSD. The only apparent exception is the first maximum of the T1 membrane. Its wide shape, however, consists of two overlapping distributions that together can indicate the presence of more pores than a single narrow distribution. The *N* value confirms this. The order of the *N* values is consistent with the earlier conclusion that small, network pores make most of the pores in the membrane skin.

All the considered details of both the PSDs and *N* values help explain the membrane performance data. First, the more numerous small, network pores, and correspondingly higher first maximum in the pore size distributions are responsible for the higher permeation rates of water Q_w and salt solution Q of the membranes. Whereas the permeation rates are primarily determined by the fraction of the small, network pores, a contribution of the bigger, aggregate pores (the location and size of the "second" distribution) to the membrane rejection factor R is also important. The rejection factor values R are determined by both the locations and heights of the first, network pore distributions and the second, aggregate pore distributions.

For example, the T2 and D2 membrane samples show the comparable rejection factors due to the composite influence of these two sets of data. The influence of the locations and sizes of the network pore distributions in these membranes is practically compensated by the locations and sizes of the aggregate pore distributions giving ultimately the almost same rejection factor values. Further, the D1 membrane sample shows the highest sodium chloride rejection factor, R value, because in addition to the reasonable number of small pores its second distribution is located at 1.0 nm, the lowest aggregate pores location of all four membranes. The relatively small aggregate pores do not allow significant solute permeation, i.e. the membrane's rejection factor is high.

The lowest rejection factor value of the T3 membrane sample can be explained by the membrane's smallest effective number of pores combined with the aggregate pores distribution located at fairly large dimensions and the appearance of a number of medium-size pores. The two latter groups of pores enable the enhanced salt permeation and consequently low rejection factor value. The pore size distribution of the T1 membrane shows the similar aggregate pores' location

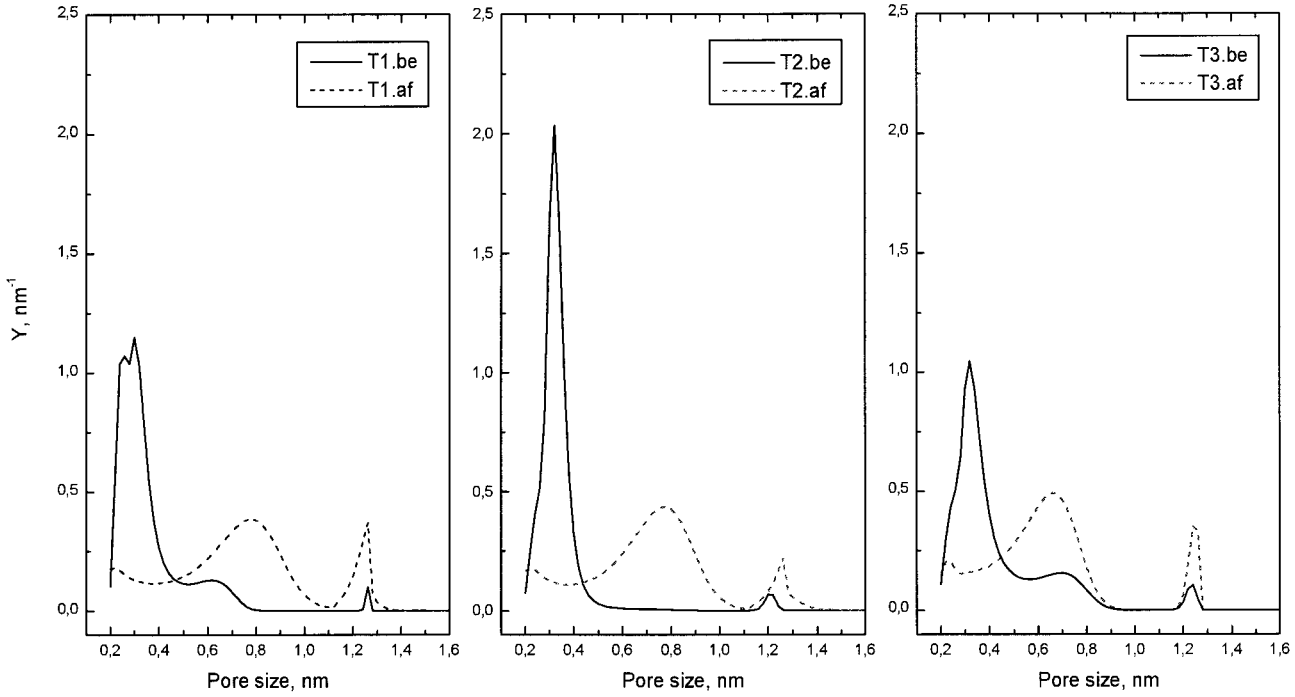

Figure 2 Pore size distributions of the cellulose triacetate membrane samples before and after hydrolysis.

and the second maximum height together with the presence of the medium-size pores. However, these "negative" features are compensated by the abundance of network pores (wide, double first peak in PSD) giving eventually the reasonable rejection factor value, $R = 0.864$.

Effect of Hydrolysis

A problem arising in the PSD determination of the membranes after hydrolysis is an unknown extent of the hydrolysis process in the membrane skin. McCray et al.[6] reported that the rate of hydrolysis in the dense skin is much slower than the rate in the porous sublayer, and it seems reasonable to say that the process of hydrolysis in the dense skin was not completed. If the hydrolysis is the first-order rate process,[2,3] it could be estimated that after 90 h of hydrolysis, the acetyl content in the upper layer of the CDA membranes is approximately 32%, and that in the CTA membranes 39%. Therefore, the PSD in the membrane skin after hydrolysis in this study were calculated using the surface force parameters of different markers for the cellulose acetate of the fairly low degree of acetylation,[10] cellulose acetate material of acetyl content 31.8%. The results in form of the membrane PSD curves obtained by such calculation for the examined CTA and the CDA samples are given in Figures 2 and 3 in comparison with the corresponding PSD curves of the original membrane samples.

Figures 2 and 3 show that the PSD of all the membranes after the hydrolysis differ remarkably from the PSD of the original membrane samples. The first maxima of the PSD of all the membranes after the hydrolysis are significantly lower and located at the greater pore size, between 0.8 and 0.9 nm. The second, aggregate pores distribution of the CTA membranes is noticeably enlarged and, in the case of CDA membranes, it is shifted toward greater pores.

The calculated effective numbers of pores in the upper surface of the membranes after hydrolysis are listed in the second column of Table III. The data obtained show a noticeable decrease in the effective number of pores in all the membranes. The change caused by the hydrolysis is primarily attributed to the drastic decrease of the effective number of the smaller, network pores.

The results on the transformations taking place in the membrane skin during hydrolysis can

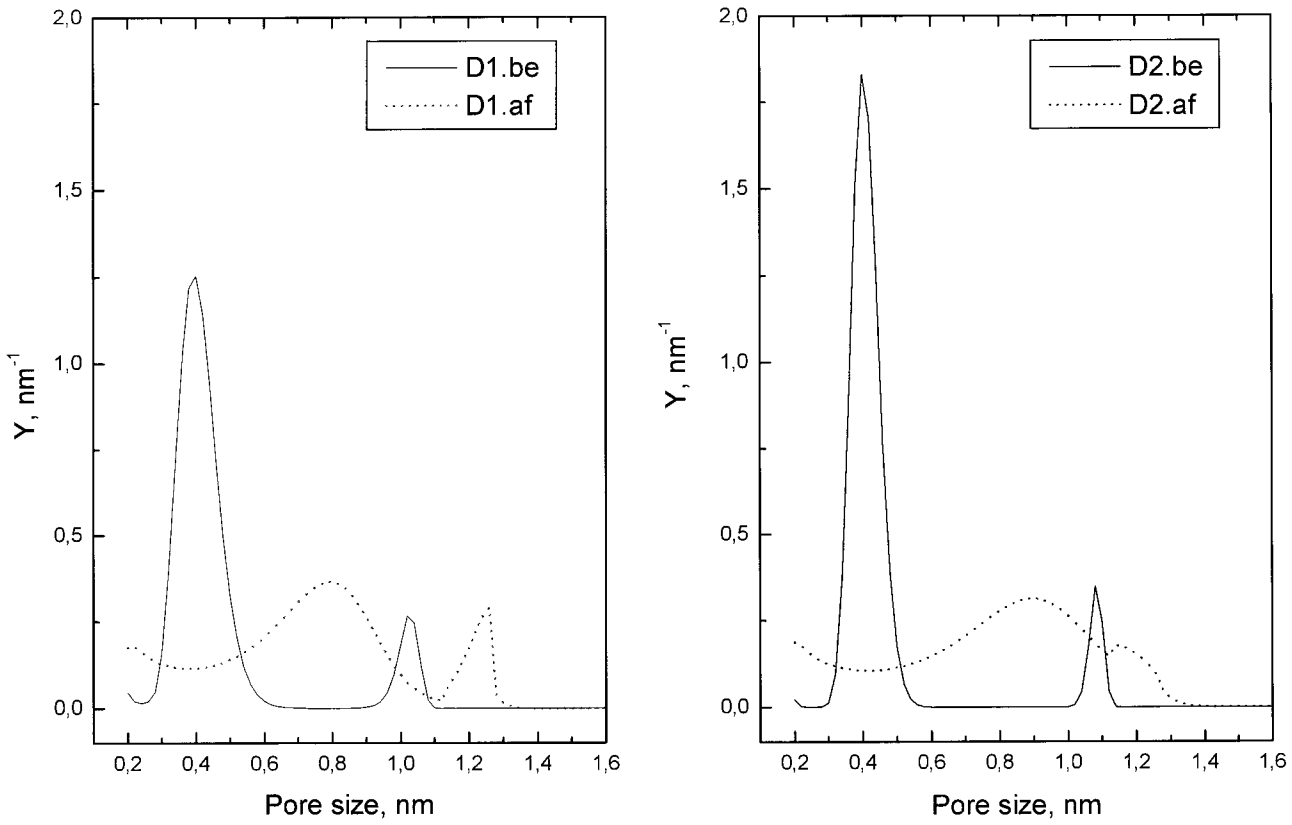

Figure 3 Pore size distributions of the cellulose diacetate membrane samples before and after hydrolysis.

be explained in terms of the concept of "pore" described earlier. The transport paths of the solute and solvent molecules through the membrane's skin are the open pores and/or the continuous interconnecting pore network. The effective number and perhaps the size of "active" pores are influenced by changes in the membrane material caused by the hydrolysis reaction with the alkaline buffer solution. A lot of the network pores in the skin is obviously closed by the hydrolysis reaction, decreasing the overall effective number of pores. In addition, the dimensions of the rest of the smallest pores increase owing to the chemical attack on the membrane matrix making them more permeable to both water and the solutes. Such changes evidently reflect in the membrane performance parameters, primarily in a decrease of the rejection factor values. The increase in the permeation rates values, Q_w and Q, is gentler because of two counteracting effects: the permeation rates increase due to the enlarged fraction of the wide aggregate pores, and their decrease caused by the remarkably diminished number of the network pores.

CONCLUSIONS

From the results of membrane performance and membrane porosity determinations described above, the following conclusions can be drawn:

1. The different values of the asymmetric cellulose acetate membrane performance parameters are explained on the basis of the membrane porosity parameters, the pore size distribution, and the effective number of pores in the membranes' skin.
2. The membrane performance parameters, the solute rejection factor, and the solute and solvent permeation rates change due to the alkaline hydrolysis of cellulose acetate membrane material. The decrease of the rejection factor values and the increase of the permeation rates are attributed to the closing of a part of the network pores and to the simultaneous increase of the rest of the pores in the membrane skin.

APPENDIX

Table A.I Comparison of Experimental and Calculated Rejection Factors *R* of the Examined Membranes Before Hydrolysis[a]

Membrane	1,3-Dioxolane	1,4-Dioxane	Oxepane	12-Crown-4	15-Crown-5	18-Crown-6
T1	0.24 (0.21)	0.27 (0.31)	0.43 (0.37)	0.80 (0.81)	0.82 (0.83)	0.82 (0.84)
T2	0.12 (0.12)	0.18 (0.20)	0.41 (0.31)	0.78 (0.80)	0.77 (0.83)	0.87 (0.84)
T3	0.19 (0.18)	0.24 (0.28)	0.56 (0.35)	0.82 (0.83)	0.78 (0.83)	0.80 (0.84)
D1	0.17 (0.18)	0.33 (0.34)	0.73 (0.52)	0.88 (0.84)	0.83 (0.92)	0.88 (0.92)
D2	0.11 (0.11)	0.23 (0.25)	0.61 (0.43)	0.85 (0.79)	0.86 (0.90)	0.82 (0.90)

[a] Calculated data in parentheses.

Table A.II Comparison of Experimental and Calculated Rejection Factors *R* of the Examined Membranes After Hydrolysis[a]

Membrane	1,3-Dioxolane	1,4-Dioxane	Oxepane	12-Crown-4	15-Crown-5	18-Crown-6
T1	0.15 (0.14)	0.21 (0.23)	0.42 (0.38)	0.77 (0.76)	0.85 (0.86)	0.82 (0.86)
T2	0.15 (0.14)	0.23 (0.23)	0.35 (0.35)	0.79 (0.74)	0.80 (0.84)	0.86 (0.85)
T3	0.15 (0.14)	0.18 (0.20)	0.48 (0.34)	0.73 (0.70)	0.75 (0.80)	0.76 (0.80)
D1	0.15 (0.15)	0.23 (0.25)	0.46 (0.40)	0.79 (0.78)	0.87 (0.87)	0.82 (0.87)
D2	0.10 (0.10)	0.19 (0.20)	0.36 (0.33)	0.77 (0.69)	0.80 (0.79)	0.72 (0.80)

[a] Calculated data in parenthesis.

REFERENCES

1. Kesting, R. E. In Reverse Osmosis and Synthetic Membranes; Sourirajan S., Ed.; National Research Council Canada: Ottawa, 1977; p 106.
2. Vos, K. D.; Hatcher, A. P.; Merten, U. Ind Eng Chem Prod Res Dev 1966, 5, 211.
3. Sammon, D. C.; Stringer, B.; Stephen, I.G. Presented at the 5th International Symposium on Fresh Water from the Sea; Alghero, Italy, 1976; Vol 4, p 179.
4. Spatz D. D.; Friedlander R.H. Osmonics, Inc; 1977, Aug.10.
5. Glater, J.; McCray, S. B, Desalination 1983, 46, 389.
6. McCray, S. B.; Vilker, V. L.; Nobe, K. J Membr Sci 1991, 59, 305.
7. Matsuura T.; Sourirajan, S. Ind Eng Chem Process Des Dev 1981, 20, 273.
8. Chan, K.; Matsuura, T.; Sourirajan S. Ind Eng Chem Prod Res Dev 1982, 21, 605.
9. Chan, K.; Tinghui, L.; Matsuura, T.; Sourirajan, S. Ind Eng Chem Prod Res Dev 1984, 23, 124.
10. Nguyen, T. D.; Chan, K.; Matsuura, T.; Sourirajan, S. Ind Eng Chem Prod Res Dev 1984, 23, 501.
11. Kastelan-Kunst, L.; Dananic, V.; Kunst, B.; Kosutic, K. J Membr Sci 1996, 109, 223.
12. Kosutic, K.; Kastelan-Kunst, L.; Kunst, B. J Membr Sci 2000, 168, 101.